

No Detectable Kilonova Counterpart is Expected for O3 Neutron Star–Black Hole Candidates

JIN-PING ZHU ¹, SHICHAO WU ², YUAN-PEI YANG ³, BING ZHANG ⁴, YUN-WEI YU ⁵, HE GAO ²,
ZHOUJIAN CAO ² AND LIANG-DUAN LIU ²

¹*Department of Astronomy, School of Physics, Peking University, Beijing 100871, China*

²*Department of Astronomy, Beijing Normal University, Beijing 100875, China*

³*South-Western Institute for Astronomy Research, Yunnan University, Kunming, Yunnan, People's Republic of China*

⁴*Department of Physics and Astronomy, University of Nevada, Las Vegas, NV 89154, USA*

⁵*Institute of Astrophysics, Central China Normal University, Wuhan 430079, China*

ABSTRACT

We analyse the tidal disruption probability of potential neutron star–black hole (NSBH) merger gravitational wave (GW) events, including GW190426.152155, GW190814, GW200105.162426 and GW200115.042309, detected during the third observing run of the LIGO/Virgo Collaboration, and the detectability of kilonova emission in connection with these events. The posterior distributions of GW190814 and GW200105.162426 show that they must be plunging events and hence no kilonova signal is expected from these events. With the stiffest NS equation of state allowed by the constraint of GW170817 taken into account, the probability that GW190426.152155 and GW200115.042309 can make tidal disruption is $\sim 24\%$ and $\sim 3\%$, respectively. However, the predicted kilonova brightness is too faint to be detected for present follow-up search campaigns, which explains the lack of electromagnetic (EM) counterpart detection after triggers of these GW events. Based on the best constrained population synthesis simulation results, we find that disrupted events account for only $\lesssim 20\%$ of cosmological NSBH mergers since most of the primary BHs could have low spins. The associated kilonovae for those disrupted events are still difficult to be discovered by LSST after GW triggers in the future, because of their low brightness and larger distances. For future GW-triggered multi-messenger observations, potential short-duration gamma-ray bursts and afterglows are more probable EM counterparts of NSBH GW events.

Keywords: Gravitational waves (678), Neutron stars (1108), Black holes (162)

1. INTRODUCTION

Mergers of binary neutron star (BNS) and neutron star–black hole (NSBH) have been proposed to be progenitors of short-duration gamma-ray bursts (sGRBs; Eichler et al. 1989; Paczyński 1991; Narayan et al. 1992), source of heavy elements (Lattimer & Schramm 1974, 1976) and kilonovae (Li & Paczyński 1998; Metzger et al. 2010). On 2017 August 17th, a gravitational wave (GW) signal from a binary neutron star (BNS) merger event (GW170817; Abbott et al. 2017a) was first identified by the GW detectors of LIGO and Virgo. Subsequent data analyses revealed that this BNS GW event was associated with a sGRB (GW170817A; Abbott et al. 2017b; Goldstein et al. 2017; Savchenko et al. 2017; Zhang et al. 2018), a fast-evolving ultraviolet-optical-infrared transient (AT2017gfo; e.g., Abbott et al. 2017c; Arcavi et al. 2017; Coulter et al. 2017; Drout et al. 2017; Evans et al. 2017; Kasliwal et al. 2017; Pian et al. 2017; Smartt et al. 2017; Kilpatrick et al. 2017), and a broadband off-axis jet afterglow (Margutti et al. 2017; Troja et al. 2017; Lazzati et al. 2018; Lyman et al. 2018; Ghirlanda et al. 2019). The fast-evolving transient was well explained by the theoretical predictions of kilonova emission (Li & Paczyński 1998; Metzger et al. 2010). The joint observations of the GW signal of this BNS event and its associated electromagnetic (EM) counterparts provided the smoking-gun evidence for the long-hypothesized origin of sGRBs and kilonovae.

The multi-messenger observations of GW170817 provided an ideal paragon for GW-led follow-up searches of EM signals. With the successful detection of a GW signal and its associated EM counterparts from a BNS merger, one may especially expect to catch as-yet undiscovered GW signals from neutron star–black hole (NSBH) mergers and search for their associated kilonova emissions in upcoming observing runs for the LIGO/Virgo collaboration (LVC). During the third observing run (O3) of LVC, several GW alerts for compact binary coalescence (CBC) with at least one NS member in the merger system (i.e., either BNS or NSBH mergers) have been issued. However, in spite of many efforts for follow-up observations, no confirmed EM counterpart candidate was identified¹ (e.g., Anand et al. 2020; Andreoni et al. 2020; Coughlin et al. 2020a; Gompertz et al. 2020; Page et al. 2020; Kasliwal et al. 2020; Sagués Carracedo et al. 2020; Becerra et al. 2021). Kawaguchi et al. (2020a); Fragione & Loeb (2021) gave a constraint on the NS mass-radius relationship based on the observed results of no confirmed counterpart for NSBH candidates. One plausible explanation for the lack of detection of an EM counterpart is that present EM searches are too shallow to achieve distance and volumetric coverage for the probability maps of LVC events (Coughlin et al. 2020b; Sagués Carracedo et al. 2020; Zhu et al. 2020b). However, it is also possible and even likely that the EM counterparts are intrinsically missing, e.g. for NSBH mergers there might not be material left outside of the merged BH remnant since the NS is not tidally disrupted but is swallowed as a whole into the BH (i.e. the so-called “plunging” event) (Zhu et al. 2020b).

Very recently, the observations of four CBC GW events in O3 of LVC with component masses potentially consistent with NSBH binaries have been reported. These four potential NSBH events are GW190426_152155 (Abbott et al. 2020a), GW190814² (Abbott et al. 2020b), GW200105_162426, and GW200115_042309 (Abbott et al. 2021), abbreviated as GW190426, GW190814, GW200105, and GW200115 hereafter. Many detailed follow-up observations for these GW events show no possible associated EM counterpart (e.g., Hosseinzadeh et al. 2019; Goldstein et al. 2019b; Anand et al. 2020; Thakur et al. 2020; Kilpatrick et al. 2021; Alexander et al. 2021). In this paper, we analyse the tidal disruption probability of these four NSBH GW events to investigate why their associated EM signals were not detected by the follow-up observations. Moreover, by combining population synthesis results, we assess the detectability of NSBH EM counterparts for future GW-triggered follow-up observations.

2. TIDAL DISRUPTION AND KILONOVA DETECTABILITY

2.1. *Fitting Formulas for the Remnant Mass and Dynamical Ejecta Mass*

Whether a NS can be tidally disrupted by the primary BH and eject a certain amount of material could be determined by the relative positions between the radius of the BH innermost stable circular orbit (ISCO) R_{ISCO} and the NS tidal disruption radius R_{tidal} (e.g., Kyutoku et al. 2011; Shibata & Taniguchi 2011; Foucart 2012). The former depends on the primary BH mass M_{BH} and the dimensionless spin parameter projected onto the orientation of orbital angular momentum χ_{BH} . One can give the normalized ISCO radius $\tilde{R}_{\text{ISCO}} = c^2 R_{\text{ISCO}} / GM_{\text{BH}}$ (Bardeen et al. 1972), i.e., $\tilde{R}_{\text{ISCO}} = 3 + Z_2 - \text{sign}(\chi_{\text{BH}}) \sqrt{(3 - Z_1)(3 + Z_1 + 2Z_2)}$, with $Z_1 = 1 + (1 - \chi_{\text{BH}}^2)^{1/3}[(1 + \chi_{\text{BH}})^{1/3} + (1 - \chi_{\text{BH}})^{1/3}]$ and $Z_2 = \sqrt{3\chi_{\text{BH}}^2 + Z_1^2}$. The radius at which tidal disruption occurs, in the Newtonian approximation, can be expressed as $R_{\text{tidal}} \sim R_{\text{NS}}(3M_{\text{BH}}/M_{\text{NS}})^{1/3}$ which is a function of BH mass M_{BH} , NS mass M_{NS} , and NS radius R_{NS} . For a NS with a certain mass M_{NS} , its radius R_{NS} and compactness $C_{\text{NS}} = GM_{\text{NS}}/c^2 R_{\text{NS}}$ are dependent on the NS equation of state (EoS).

When a NS is tidally disrupted, numerical relativity (NR) simulations (e.g., Foucart et al. 2013; Kyutoku et al. 2013, 2015) showed that plenty of materials would remain outside the remnant BH to form a disk and an unbound tidal tail. In order to judge whether or not tidal disruption happens for a GW event, evaluation of the amount of total baryon mass after NSBH mergers could be an important quantitative diagnostic. Foucart et al. (2018) (hereafter F18) adopted an empirical model to estimate the total amount of remnant masses $M_{\text{total,fit}}$ outside the BH horizon as a non-linear function of ISCO radius and tidal disruption radius with the consideration of 75 NR simulations. The model of F18 gives

$$\frac{M_{\text{total,fit}}}{M_{\text{NS}}^{\text{b}}} = \left[\max \left(\alpha \frac{1 - 2C_{\text{NS}}}{\eta^{1/3}} - \beta \tilde{R}_{\text{ISCO}} \frac{C_{\text{NS}}}{\eta} + \gamma, 0 \right) \right]^{\delta}, \quad (1)$$

¹ Goldstein et al. (2019a) reported a sub-threshold GRB candidate, GBM-190816, which was potentially associated with a sub-threshold LVC compact binary coalescence candidate. Yang et al. (2020) investigated the physical implications of this potential association and indicated this GW candidate could be a NSBH merger with the mass ratio $Q = 2.26_{-1.43}^{+2.75}$. Li & Shen (2021) showed this event could have a large effective spin. However, since both the GW candidate and sGRB candidate were sub-threshold, the case was not confirmed.

² GW190814’s secondary component of mass lies in the range of $2.50 - 2.67 M_{\odot}$ which is at a high confidence level above the maximum allowed mass of a NS (The LIGO Scientific Collaboration et al. 2020a), but the possibility of a NS secondary component cannot be excluded (e.g., Godzieba et al. 2020; Zhang & Li 2020). Therefore, we still include this event in our discussion.

where $\alpha = 0.406$, $\beta = 0.139$, $\gamma = 0.255$, $\delta = 1.761$, M_{NS}^{b} is the baryonic mass of the NS, $\eta = Q/(1+Q)^2$, and $Q = M_{\text{BH}}/M_{\text{NS}}$ is the mass ratio between the BH mass and the NS mass. The more accurate application range of this formula is $Q \in [1, 7]$, $\chi_{\text{BH}} \in [-0.5, 0.9]$, and $C_{\text{NS}} \in [0.13, 0.182]$ (Foucart et al. 2018). A zero $M_{\text{total,fit}}$ corresponds to no tidal disruption, which means that the NSBH merger is a plunging event.

Similarly, based on F18, Zhu et al. (2020a) (hereafter Z20) presented a similar formula for tidal dynamical ejecta mass by considering 66 NR simulations. The fitting parameters are $\alpha = 0.218$, $\beta = 0.028$, $\gamma = -0.122$, and $\delta = 1.358$. The formula covers the accurate range of $Q \in [1, 7]$, $\chi_{\text{BH}} \in [-0.05, 0.9]$, and $C_{\text{NS}} \in [0.108, 0.18]$. In addition, Kawaguchi et al. (2016) (hereafter K16) and Krüger & Foucart (2020) (hereafter KF20) also provided fitting formulas to model the dynamical ejecta mass.

We note that the fittings of NR simulations ignored the effects of precession, NS spin, and orbital eccentricity. Since the fitting formulas of the total remnant mass and the dynamical ejecta mass are obtained with independent NR data, one needs to set an upper limit on the maximum fraction of dynamical ejecta mass to the total remnant mass, i.e., $M_{\text{d,max}} = f_{\text{max}} M_{\text{total,fit}}$. We set $f_{\text{max}} \approx 0.5$ based on NR simulation results (Kyutoku et al. 2015). Therefore, the final empirical mass of the dynamical ejecta is $M_{\text{d}} = \min(M_{\text{d,fit}}, f_{\text{max}} M_{\text{total,fit}})$.

2.2. Source Properties and Tidal Disruption Probability

Table 1. Source properties for potential NSBH events

GW Event	GW190426	GW190814	GW200105	GW200115
Primary mass M_1/M_{\odot}	$5.7^{+3.9}_{-2.3}$	$23.2^{+1.1}_{-1.0}$	$8.9^{+1.1}_{-1.3}$	$5.9^{+1.4}_{-2.1}$
Secondary mass M_2/M_{\odot}	$1.5^{+0.8}_{-0.5}$	$2.59^{+0.08}_{-0.09}$	$1.9^{+0.2}_{-0.2}$	$1.4^{+0.6}_{-0.2}$
Mass ratio $Q = M_1/M_2$	$4.2^{+6.7}_{-2.7}$	$8.9^{+0.8}_{-0.6}$	$4.8^{+1.1}_{-1.1}$	$4.2^{+2.1}_{-2.3}$
Effective inspiral spin χ_{eff}	$-0.03^{+0.32}_{-0.30}$	$-0.002^{+0.060}_{-0.061}$	$-0.01^{+0.08}_{-0.12}$	$-0.14^{+0.17}_{-0.34}$
Luminosity distance D_{L}/Mpc	370^{+190}_{-160}	241^{+41}_{-45}	280^{+110}_{-110}	310^{+150}_{-110}

NOTE—Combined source properties of four potential NSBH events inferred from low-spin priors of the secondary component. We report the median values with 90% credible intervals.

References: GW190426 (Abbott et al. 2020a), GW190814 (Abbott et al. 2020b), GW200105, and GW 200115 (Abbott et al. 2021).

The physical properties of the four GW events using the methodology of a coherent Bayesian analysis (Abbott et al. 2019a) have been released recently. It is plausibly expected that most NSs would have low spins before NSBH mergers since NSs would have spun down via magnetic dipole radiation during the long history in the pre-merger phase. This has been suggested by both pulsar observations (e.g., Manchester et al. 2005) and population synthesis models (e.g., Kiel et al. 2008; Osłowski et al. 2011). Therefore, we only collect the posterior samples of binary parameters with consideration of a low-spin prior assumption. The posterior results of these four events are shown in Table 1. In order to calculate the tidal disruption probability, we need to know χ_{BH} and the EoS. We use the primary’s aligned spin components (i.e., χ_{1z}) in the posterior samples to estimate χ_{BH} . For the NS EoS, these four potential NSBH GW events have poor measurements for tidal deformability (Abbott et al. 2021) so that EoS cannot be constrained directly. Abbott et al. (2021) adopted the method presented by Stachie et al. (2021) to marginalize over the EoSs when calculating the ejecta mass for GW200105 and GW200115, and showed that their ejecta masses are essentially negligible. In our work, we select three specific representative EoSs from soft to stiff as shown in Figure 1, including AP4 (Akmal & Pandharipande 1997), DD2 (Typel et al. 2010), and Ms1 (Müller & Serot 1996). Among them, AP4 is one of the most likely EoS while DD2 is permitted as one of the stiffest EoS constrained by GW170817 (Abbott et al. 2018, 2019b) and Dietrich et al. (2020). One can thus calculate the NS baryonic mass M_{NS}^{b} as a function of M_{NS} introduced by Gao et al. (2020):

$$M_{\text{NS}}^{\text{b}} = M_{\text{NS}} + A_1 \times M_{\text{NS}}^2 + A_2 \times M_{\text{NS}}^3, \quad (2)$$

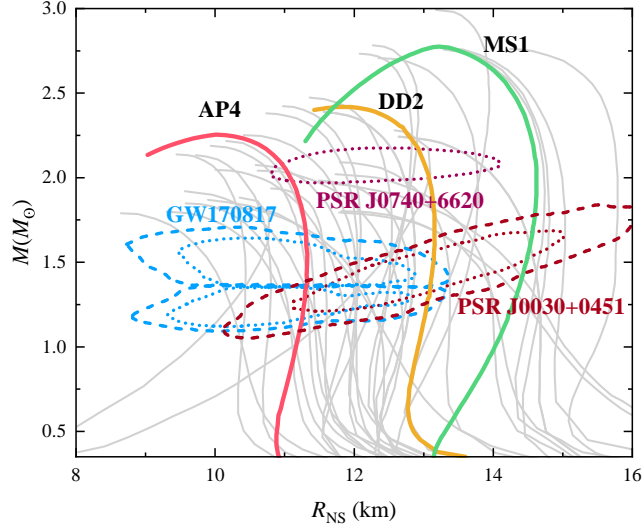


Figure 1. Observational constraints on the mass-radius relationship of selected sources, compared with NS EoS models. The blue, dark violet, and carmine are observational constraints by the GW170817 (Abbott et al. 2018, dotted contours at 68% and dashed contours at 95% confidence levels), NICER measurement of PSR J0740+6620 (Miller et al. 2021, 68% confidence level), and NICER measurement of PSR J0030+0451 (Riley et al. 2019, dotted contours at 68% and dashed contours at 95% confidence levels) (see Dietrich et al. 2020, who used more observational limits to constrain the mass-radius relationship). Colored solid lines are the three selected representative EoSs used in this work. Other EoSs (gray solid lines) are obtained from Bauswein et al. (2012, 2013).

Table 2. Characteristic Parameters for the Selected EoSs

EoS	M_{TOV}/M_{\odot}	A_1	A_2
AP4	2.22	0.045	0.023
DD2	2.42	0.046	0.014
Ms1	2.77	0.042	0.010

NOTE—The columns from left to right represent the NS EoSs we selected, the NS TOV mass M_{TOV} , and best fit values of A_1 and A_2 for each EoS in Equation (2). All the values of each parameter are cited from Gao et al. (2020).

where A_1 and A_2 for each selected EoS are presented in Table 2, and M_{NS}^b and M_{NS} in this formula are in units of M_{\odot} . We estimate the compactness of NS based on the empirical formula given by Coughlin et al. (2017)

$$C_{\text{NS}} = 1.1056 \times (M_{\text{NS}}^b/M_{\text{NS}} - 1)^{0.8277}. \quad (3)$$

Figure 2 shows the parameter space where the NS can be tidally disrupted using the F18 model. The tidal disruption tends to occur if the NSBH binaries have a low-mass NS component with a stiff EoS, and a high-spin low-mass BH component. In particular, the parameter space would significantly increase if the primary BH has a larger χ_{BH} value. If the BH component carries a low spin or even has an opposite spin with respect to the orbital angular momentum (like O3 LVC NSBH candidates), the mass space that allows tidal disruption of the NS would be limited.

We also show the posterior distribution for the component masses of the O3 LVC NSBH candidates in Figure 2. The explicit results of tidal disruption probabilities for these four events are collected in Table 3. It is obvious that there is no probability for GW190814 (if it is a NSBH) and GW200105 to have tidal disruption, so no EM signals are expected following these two merger events. The probability for GW200115 to have material outside of the remnant BH horizon is also small, unless the EoS of NS component is extremely stiff. GW190426 is the most likely event for tidal disruption. In view that DD2 is one of the stiffest EoS allowed by the observations of GW170817 (Abbott et al. 2019b), the probability could be smaller than $\lesssim 24\%$.

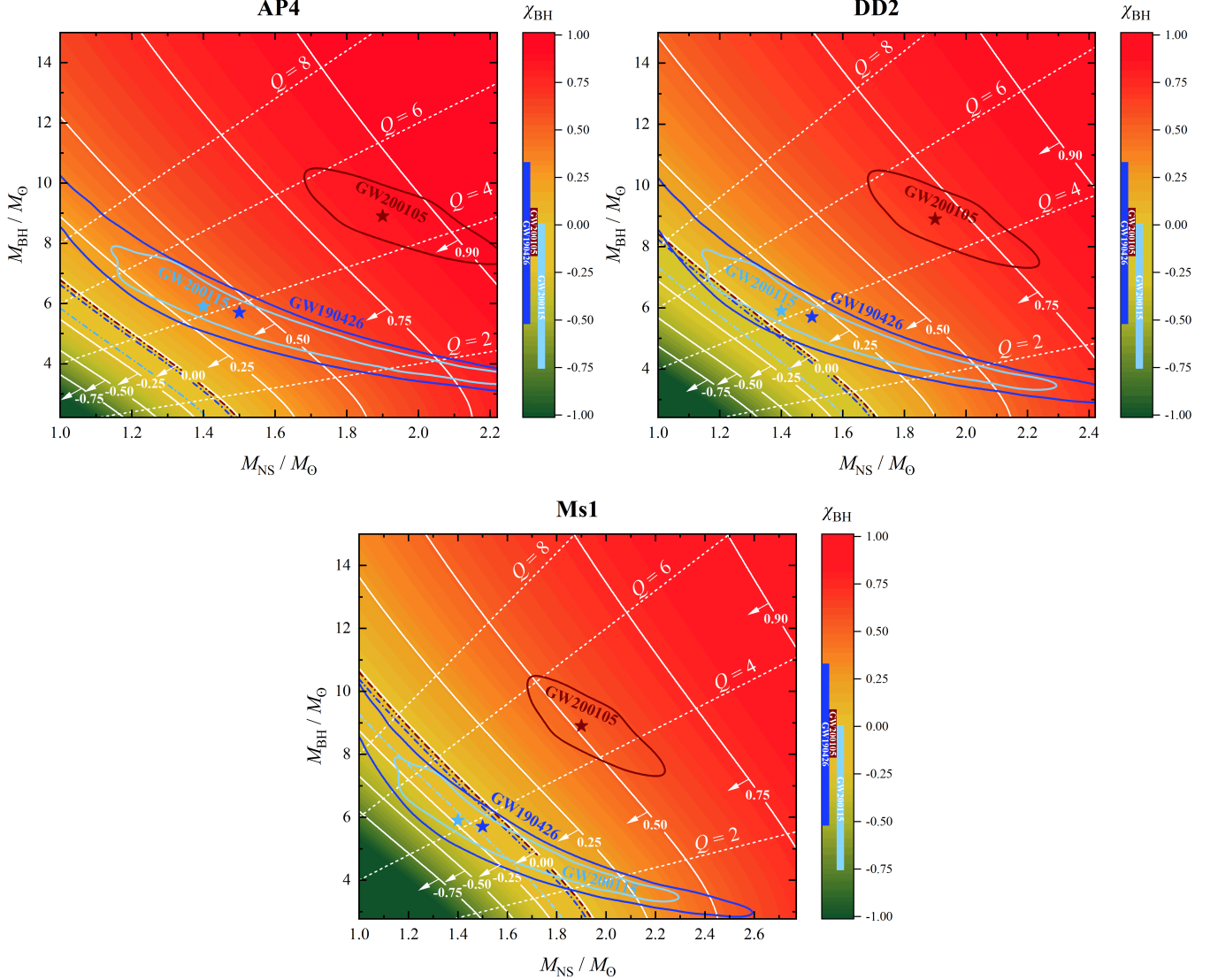


Figure 2. The source-frame mass parameter space for NSBH merger systems to allow tidal disruption of the NS by the BH. Three EoSs are considered: AP4 (top left panel), DD2 (top right panel), and Ms1 (bottom panel). The dashed lines represent mass ratio $Q = M_{\text{BH}}/M_{\text{NS}}$ from $Q = 2$ to $Q = 8$. We mark several values of primary BH spin along the orbital angular momentum from $\chi_{\text{BH}} = -0.75$ to $\chi_{\text{BH}} = 0.90$ as solid lines in each panel. For a specific χ_{BH} , the NSBH mergers with component masses located at the bottom left parameter space (denoted by the direction of the arrows) can allow tidal disruptions to occur. For GW190426 (dark blue), GW200105 (brown), and GW200115 (light blue), the 90% credible posterior distributions (colored solid lines) and the medians (colored star points) are displayed. Corresponding median values of χ_{BH} for these three sources are marked as dashed-dotted lines while their 90% posterior distributions are labeled at the dextral color bars of each panel.

2.3. Dynamical Ejecta Mass and Luminosity Distributions

Table 3. Tidal disruption probability and dynamical ejecta mass distribution

GW Event	EoS	P_{NSBH}^a	Tidal Disruption Probability		Dynamical Ejecta Mass ^b		
			F18		K16	KF20	Z20
GW190426	AP4	94.4%	5.95%		$1.9_{-1.8}^{+6.1} \times 10^{-3} M_{\odot}$	$5.3_{-4.8}^{+8.7} \times 10^{-3} M_{\odot}$	$1.7_{-1.7}^{+6.2} \times 10^{-3} M_{\odot}$
	DD2	97.6%	24.3%		$7_{-6}^{+16} \times 10^{-3} M_{\odot}$	$10_{-9}^{+14} \times 10^{-3} M_{\odot}$	$5_{-5}^{+17} \times 10^{-3} M_{\odot}$
	Ms1	99.8%	65.2%		$1.5_{-1.3}^{+3.3} \times 10^{-2} M_{\odot}$	$1.5_{-1.2}^{+3.4} \times 10^{-2} M_{\odot}$	$1.3_{-1.2}^{+3.4} \times 10^{-2} M_{\odot}$
GW190814	AP4	0%	—		—	—	—
	DD2	0.30%	0%		0	0	0
	Ms1	99.9%	0%		0	0	0
GW200105	AP4	97.0%	0%		0	0	0
	DD2	99.1%	0%		0	0	0
	Ms1	99.8%	0%		0	0	0
GW200115	AP4	98.1%	0%		0	0	0
	DD2	100%	2.76%		$6_{-6}^{+39} \times 10^{-4} M_{\odot}$	$34_{-33}^{+41} \times 10^{-4} M_{\odot}$	$6_{-6}^{+39} \times 10^{-4} M_{\odot}$
	Ms1	100%	49.9%		$6_{-6}^{+11} \times 10^{-3} M_{\odot}$	$7_{-5}^{+11} \times 10^{-3} M_{\odot}$	$6_{-6}^{+11} \times 10^{-3} M_{\odot}$

^aThe probability that the GW event is a NSBH merger, i.e., the primary mass $M_1 > M_{\text{TOV}}$ and the secondary mass $M_2 \leq M_{\text{TOV}}$.

^bMedian values with 90% credible intervals of dynamical ejecta mass are calculated for events parameter space that can be tidally disrupted.

NOTE—References: (1) F18 (Foucart et al. 2018); (2) K16 (Kawaguchi et al. 2016); (3) KF20 (Krüger & Foucart 2020); (4) Z20 (Zhu et al. 2020a).

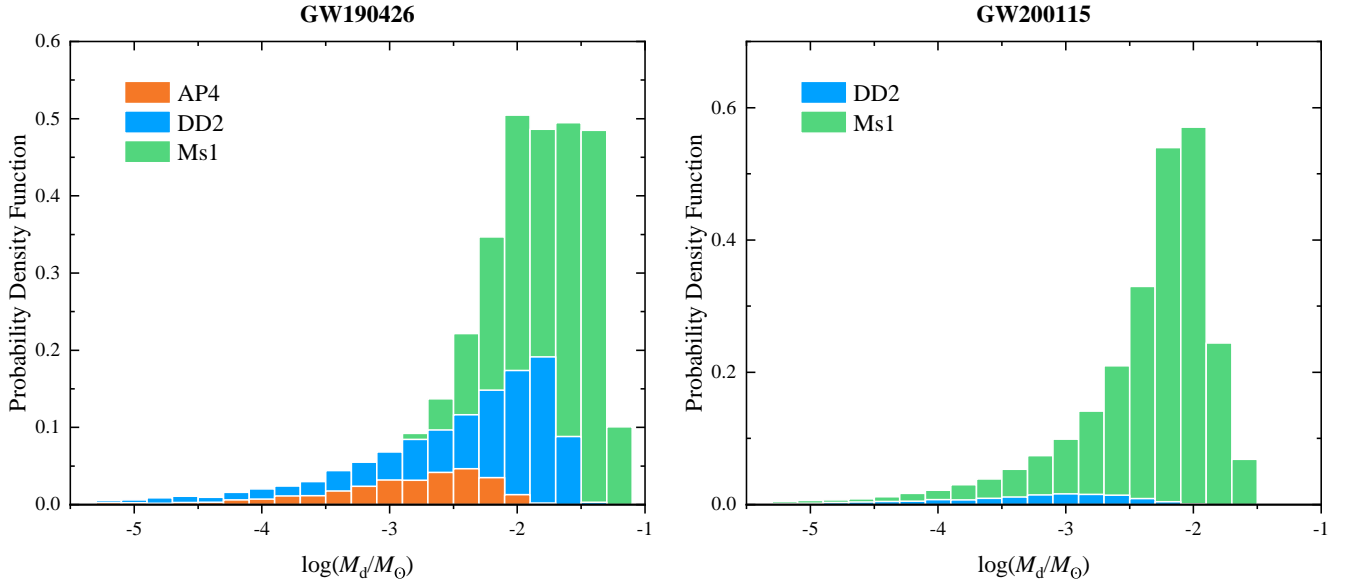


Figure 3. Probability density distributions of the dynamical ejecta mass for GW190426 (left panel) and GW200115 (right panel). The orange, blue, and green histograms represent the probability density of dynamical ejecta mass with the consideration of the EoSs AP4, DD2, and Ms1, respectively. The bin width of the histograms is set as $\Delta = 0.2$ in logarithmic scale.

Zhu et al. (2020a) showed that the fastest moving lanthanide-rich dynamical ejecta usually contribute to the majority of the NSBH kilonova emission, because the BH-torus systems formed after NSBH mergers are usually hard to produce a large amount of lanthanide-free ejecta (e.g., Fernández & Metzger 2013; Just et al. 2015; Siegel & Metzger 2017). We calculate the amount of dynamical ejecta mass for the tidal disruption parameter space of these four NSBH GW events

(see Table 3) and give the probability density distributions of the dynamical ejecta for GW190426 and GW200115 using Z20 model as shown in Figure 3. Comparing with K16 and Z20 models, the KF20 model predicts a relatively larger value for the dynamical ejecta but the difference is not too significant. The mass of the dynamical ejecta estimated by fitting the GW170817/AT 2017gfo lightcurve mainly lies in the range of $(0.01 - 0.05) M_{\odot}$ (e.g., Cowperthwaite et al. 2017; Kasen et al. 2017; Kasliwal et al. 2017; Perego et al. 2017; Tanaka et al. 2017; Villar et al. 2017). Only GW190426 has a chance to generate a similar amount of dynamical ejecta with GW 170817/AT 2017gfo if it has a NS companion with the Ms1 EoS. If the NS has an EoS of AP4 or DD2 which were not ruled out by GW170817 (Abbott et al. 2019b), the generated dynamical ejecta masses of these two NSBH GW events should be $\lesssim 10^{-2} M_{\odot}$. Even if GW190426 and GW200115 can make tidal disruption, these results indicate that the associated kilonovae would be dim.

By taking advantage of the viewing-angle dependent NSBH merger kilonova model from Zhu et al. (2020a), we show the probability density distributions of g -band and r -band peak magnitudes for GW190426 and GW200115 in Figure 4. At present, the Zwicky Transient Facility (ZTF; Graham et al. 2019) possess one of the most powerful capabilities for GW-triggered follow-up observations. The deepest 5σ observed depths of ZTF for GW200105 and GW200115 follow-up observations are $m_{AB} \approx 22$ mag reported by Anand et al. (2020). However, even though these two events could produce kilonovae, it is impossible for ZTF to observe them regardless of which EoS is adopted. We also mark the detection depths of Large Synoptic Survey Telescope (LSST; LSST Science Collaboration et al. 2009) with 30 s and 180 s exposures in Figure 4. LSST can have an enough detectability to discover the kilonova emission from GW190426 and GW200115 if the NS EoS is stiff so that the component NSs can be tidally disrupted.

3. IMPLICATIONS FROM POPULATION SYNTHESIS RESULTS

By considering several models with different common envelope treatments, stellar remnant natal kicks, cosmic chemical evolutions, and angular momentum transport mechanisms during BH formation, Belczynski et al. (2020) calculated the event rates for BNS, NSBH, and binary BH (BBH) mergers, and predicted the effective spin parameters of BBH mergers. The most recent local BNS, NSBH, and BBH merger rate densities inferred from GW observations (The LIGO Scientific Collaboration et al. 2020b; Abbott et al. 2021) are $R_{\text{BNS}} = 320^{+490}_{-240} \text{ Gpc}^{-3} \text{ yr}^{-1}$, $R_{\text{NSBH}} = 45^{+75}_{-33} \text{ Gpc}^{-3} \text{ yr}^{-1}$ (or $R_{\text{NSBH}} = 130^{+112}_{-69} \text{ Gpc}^{-3} \text{ yr}^{-1}$)³, and $R_{\text{BBH}} = 24^{+14}_{-9} \text{ Gpc}^{-3} \text{ yr}^{-1}$, respectively. The most favored population synthesis models which can match the observed merger event rates are M33.A and M43.A models (see Figure 24 and Figure 25 in Belczynski et al. 2020). The difference of these two models is due to the different assumptions of angular momentum transport mechanism during BH formation: an efficient transport by the Tayler-Spruit magnetic dynamo (MESA code; see also Qin et al. 2018) for the M33.A model, and a very-efficient transport (Fuller & Ma 2019) for the M43.A model. Both angular momentum transport models are favored to explain near-zero effective spins for the observed BBH mergers (Belczynski et al. 2020).

We combine the population synthesis simulation results of M33.A and M43.A models⁴ (Belczynski et al. 2020) and show the distributions of the source-frame masses and BH spins in Figure 5. The results reveal that the most common NSBH mergers have BH mass of $\sim (6 - 12) M_{\odot}$ and χ_{BH} of $\sim (-0.2 - 0.2)$, while the NSs in these systems have a wide range of mass distribution mainly distributed in $\sim (1.1 - 2.0) M_{\odot}$. These BH and NS mass distributions are similar to other population synthesis results (e.g., Giacobbo & Mapelli 2018; Broekgaarden et al. 2021). The median values of source-frame masses and BH spins for GW190426, GW200105, and GW200115 are basically located in the 2σ regions of population synthesis results. By adopting NS EoS of DD2, we find that only $\sim 20\%$ cosmological NSBH mergers which have less-massive BHs and less-massive NSs can allow tidal disruption to occur to produce bright kilonovae. We then simulate 5×10^6 NSBH mergers in the universe based on the population synthesis simulation results to map the distributions of r - and g -band observed peak apparent magnitudes (see Figure 6). One can conclude that the associated kilonovae for these disrupted events are still difficult to be discovered by LSST after GW triggers in the future. This is likely because most of NSBH-merger kilonovae have faint brightness and larger distances compared with BNS mergers. Via the Blandford-Znajek mechanism (Blandford & Znajek 1977), the remnant BH from these mergers can accrete from the surrounding remnant disk for disrupted events and launch a pair of collimated relativistic jets. The sGRB and afterglow would be the more promising EM counterparts of NSBH mergers for detection thanks

³ The former NSBH merger rate density was obtained under the assumption that GW200105 and GW200115 are representatives of the NSBH population, while the latter one was calculated by assuming a broader distribution of the component mass in O3 triggers (Abbott et al. 2021).

⁴ <https://www.syntheticuniverse.org/stvsgwo.php>

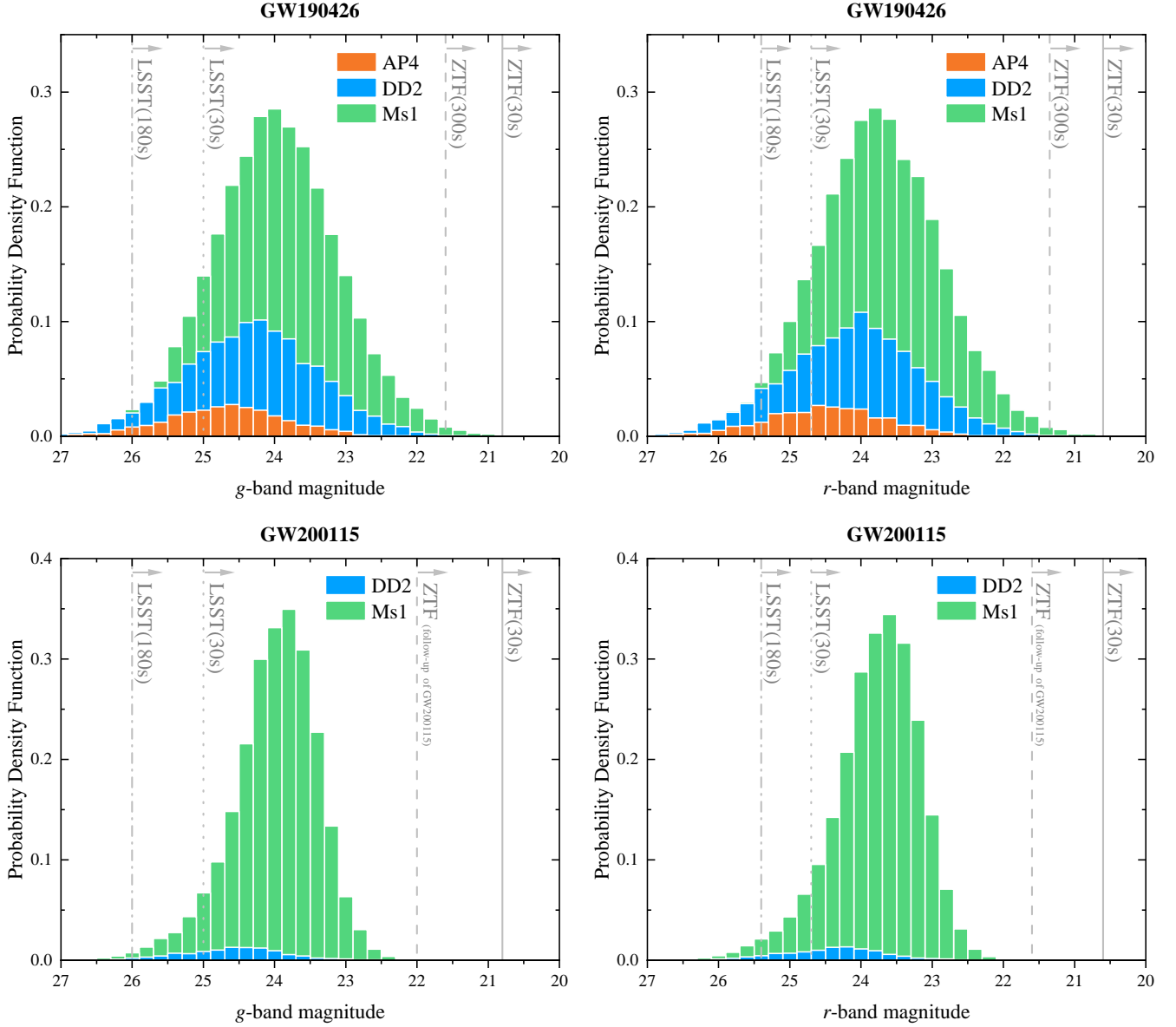


Figure 4. Probability density distributions of NSBH merger kilonova *g*-band peak magnitude (left panels) and *r*-band peak magnitude (right panels) for GW190426 (top panels) and GW200115 (bottom panels). The orange, blue, and green histograms represent the probability density of kilonova peak magnitude with the consideration of the EoSs AP4, DD2, and Ms1, respectively. The gray solid, dotted, and dashed-dotted lines show the 5σ ZTF normal survey depth, the LSST normal survey depth, and the LSST threshold depth for exposure time of 180 s under the ideal observing conditions. The ZTF deepest magnitudes for follow-up searches of GW190426 and GW200115, respectively reported by Coughlin et al. (2019); Anand et al. (2020), are marked by dashed lines. Here, the bin width of the histograms is set as $\Delta = 0.2$.

to the relativistic beaming effect of the jets. Therefore, for future GW-triggered multi-messenger observations, one may search for potential sGRBs and afterglows as plausible EM counterparts for NSBH merger GW events.

4. CONCLUSIONS AND DISCUSSION

In this paper, we have detailedly analyzed the observations of the O3 LVC NSBH merger candidates and discuss the detectability of the kilonova signals from these events. The posterior distributions revealed that the NS components in GW190814 (if it is a NSBH merger event) and GW200105 would directly plunge into their respective BH without making any EM counterpart. GW190426 and GW200115 have low probabilities for tidal disruption which are consistent with the results of LVC (Abbott et al. 2021), but even if tidal disruptions occurred, the brightness of the associated

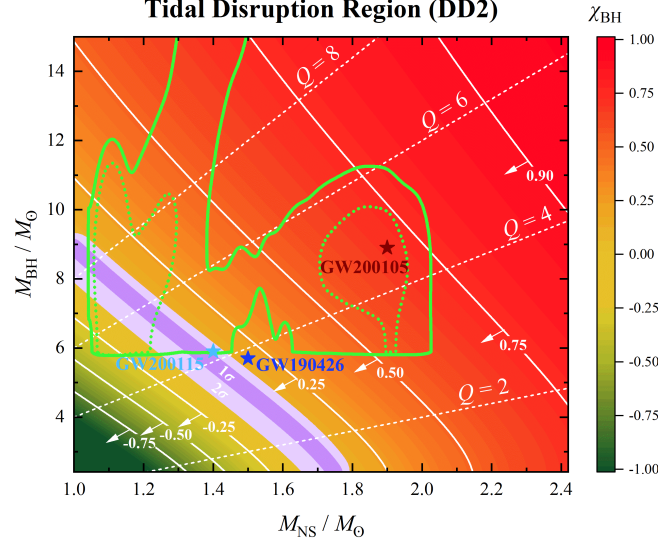


Figure 5. Similar to Figure 2 but for source-frame mass parameter space where tidal disruption can occur by considering the specific NS EoS DD2. The green dotted and solid lines represent 1σ and 2σ source-frame masses distributions of population synthesis simulations from Belczynski et al. (2020). The purple and light purple regions represent 1σ and 2σ distributions of χ_{BH} .

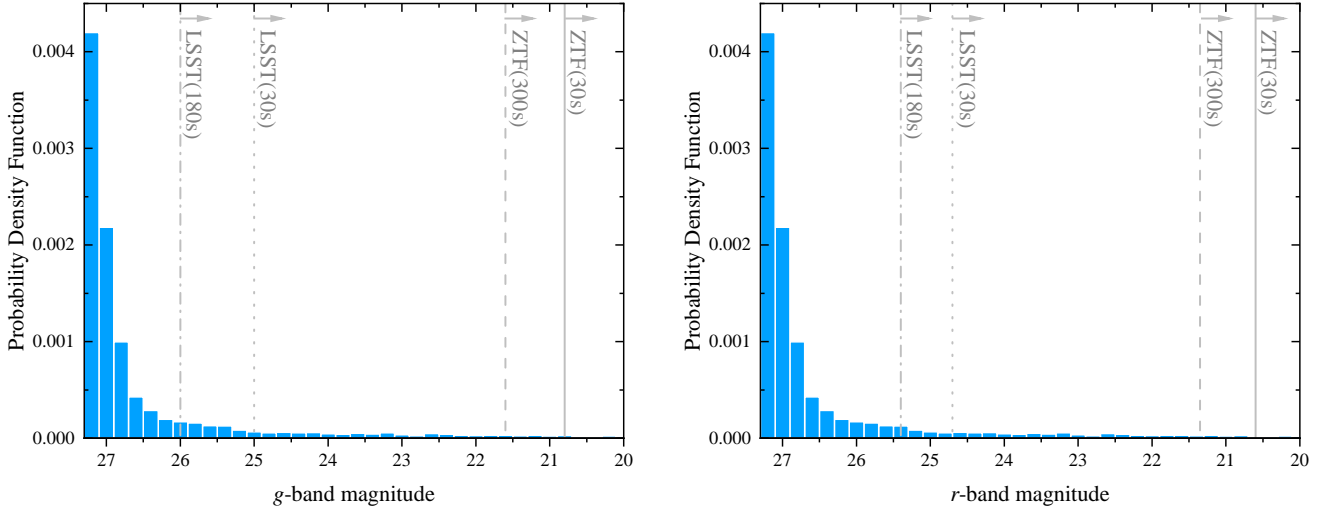


Figure 6. Probability density distributions of g -band and r -band kilonova peak apparent magnitudes for the simulated cosmological NSBH mergers. The gray solid, dashed, dotted, and dashed-dotted lines show the 5σ ZTF normal survey depth, the ZTF threshold depth for exposure time of 300s, the LSST normal survey depth, and the LSST threshold depth for exposure time of 180s under ideal observing conditions. The bin width of the histograms is set as $\Delta = 0.2$.

kilonovae of these two events could be too faint for the present follow-up survey telescopes to detect. This can thus explain why kilonovae were not found by the follow-up observations of these GW events. Considering the NS EoS of DD2 model and the best constrained population synthesis simulation results, we have found that only a small fraction ($\sim 20\%$) of cosmological NSBH mergers theoretically can occur tidal disruption and produce kilonova signals. However, the predicted brightness for most of kilonovae still be too faint for the follow-up observations of LSST. This result is basically consistent with other recent studies (e.g., Zappa et al. 2019; Zhu et al. 2020b; Drozda et al. 2020).

For future GW-triggered multi-messenger observations, one may search for potential sGRB and afterglow as ideal EM counterparts of NSBH GW events.

The kilonova model we used in this work assumes that the BH-torus cannot produce much lanthanide-poor wind ejecta (e.g., [Fernández & Metzger 2013](#); [Just et al. 2015](#); [Siegel & Metzger 2017](#)). If the electron fraction of the wind ejecta is not really low (e.g., [Fujibayashi et al. 2020a,b](#)), the NSBH kilonovae can be more luminous. We note that the differences in peak luminosity of NSBH kilonovae between the model of [Zhu et al. \(2020a\)](#) and other models (e.g., [Kawaguchi et al. 2016, 2020b](#); [Barbieri et al. 2019](#); [Darbha et al. 2021](#)) are within a factor of two, corresponding to an uncertainty of ~ 1 mag for the peak luminosity. Possible energy injection, e.g., from fallback accretion ([Rosswog 2007](#)) or Blandford-Payne mechanism ([Ma et al. 2018](#)) could also enhance the brightness of the kilonova. For these cases, future follow-up observations of NSBH merger events would be able to find a bit more associated kilonovae. However, model diversity and possible energy injection would not affect the main conclusion of this work.

Although most NSBH mergers are predicted to be plunging events, since the NSs are usually charged, some detectable EM signals, i.e., fast radio bursts or short-duration X-ray bursts, can be produced during the final merger phase for NSBH binaries ([Zhang 2019](#); [Dai 2019](#); [Sridhar et al. 2021](#)). Moreover, some CBC events are believed to be embedded in the accretion disks of active galactic nuclei (AGNs; e.g., [Cheng & Wang 1999](#); [McKernan et al. 2020](#)). The disrupted NSBH mergers in AGN disks can power sGRBs and kilonova emissions. Due to the dense atmosphere of the AGN disks, most of sGRB jets would be choked and hence it is difficult for us to observe their gamma-ray emission ([Perna et al. 2021](#); [Zhu et al. 2021c](#)). The cocoon cooling emission and kilonova emission would be outshone by the disk emission. However, one can possibly detect the cocoon shock breakout signals in the soft X-ray band and ejecta shock breakout signals in the ultraviolet band. There might be also associated high-energy neutrino emission from choked gamma-ray jets ([Zhu et al. 2021b](#)) and subsequent two shock breakouts ([Zhu et al. 2021a](#)), potentially detectable by IceCube. NSBH mergers in AGN disks are potential sources for future joint EM, neutrino, and GW multi-messenger observations.

ACKNOWLEDGMENTS

We thank Ying Qin for valuable comments. The work of J.P.Z is partially supported by the National Science Foundation of China under Grant No. 11721303 and the National Basic Research Program of China under grant No. 2014CB845800. Y.W.Y is supported by the National Natural Science Foundation of China under Grant No. 11822302, 11833003. Y.P.Y is supported by National Natural Science Foundation of China grant No. 12003028 and Yunnan University grant No.C176220100087. H.G. is supported by the National Natural Science Foundation of China under Grant No. 11690024, 12021003, 11633001. Z.J.C is supported by the National Natural Science Foundation of China (No. 11690023). L.D.L. is supported by the National Postdoctoral Program for Innovative Talents (grant No. BX20190044), China Postdoctoral Science Foundation (grant No. 2019M660515), and “LiYun” postdoctoral fellow of Beijing Normal University.

REFERENCES

- | | |
|--|---|
| <p>Abbott, B. P., Abbott, R., Abbott, T. D., et al. 2017a, <i>PhRvL</i>, 119, 161101, doi: 10.1103/PhysRevLett.119.161101</p> <p>—. 2017b, <i>ApJL</i>, 848, L13, doi: 10.3847/2041-8213/aa920c</p> <p>—. 2017c, <i>ApJL</i>, 848, L12, doi: 10.3847/2041-8213/aa91c9</p> <p>—. 2018, <i>PhRvL</i>, 121, 161101, doi: 10.1103/PhysRevLett.121.161101</p> <p>—. 2019a, <i>Physical Review X</i>, 9, 031040, doi: 10.1103/PhysRevX.9.031040</p> <p>—. 2019b, <i>Physical Review X</i>, 9, 011001, doi: 10.1103/PhysRevX.9.011001</p> | <p>Abbott, R., Abbott, T. D., Abraham, S., et al. 2020a, arXiv e-prints, arXiv:2010.14527, https://arxiv.org/abs/2010.14527</p> <p>—. 2020b, <i>ApJL</i>, 896, L44, doi: 10.3847/2041-8213/ab960f</p> <p>—. 2021, <i>ApJL</i>, 915, L5, doi: 10.3847/2041-8213/ac082e</p> <p>Akmal, A., & Pandharipande, V. R. 1997, <i>PhRvC</i>, 56, 2261, doi: 10.1103/PhysRevC.56.2261</p> <p>Alexander, K. D., Schroeder, G., Paterson, K., et al. 2021, arXiv e-prints, arXiv:2102.08957, https://arxiv.org/abs/2102.08957</p> <p>Anand, S., Coughlin, M. W., Kasliwal, M. M., et al. 2020, <i>Nature Astronomy</i>, doi: 10.1038/s41550-020-1183-3</p> |
|--|---|

- Andreoni, I., Kool, E. C., Sagues Carracedo, A., et al. 2020, arXiv e-prints, arXiv:2008.00008.
<https://arxiv.org/abs/2008.00008>
- Arcavi, I., Hosseinzadeh, G., Howell, D. A., et al. 2017, *Nature*, 551, 64, doi: [10.1038/nature24291](https://doi.org/10.1038/nature24291)
- Barbieri, C., Salafia, O. S., Perego, A., Colpi, M., & Ghirlanda, G. 2019, *A&A*, 625, A152, doi: [10.1051/0004-6361/201935443](https://doi.org/10.1051/0004-6361/201935443)
- Bardeen, J. M., Press, W. H., & Teukolsky, S. A. 1972, *ApJ*, 178, 347, doi: [10.1086/151796](https://doi.org/10.1086/151796)
- Bauswein, A., Goriely, S., & Janka, H. T. 2013, *ApJ*, 773, 78, doi: [10.1088/0004-637X/773/1/78](https://doi.org/10.1088/0004-637X/773/1/78)
- Bauswein, A., Janka, H. T., Hebeler, K., & Schwenk, A. 2012, *PhRvD*, 86, 063001, doi: [10.1103/PhysRevD.86.063001](https://doi.org/10.1103/PhysRevD.86.063001)
- Becerra, R. L., Dichiaro, S., Watson, A. M., et al. 2021, arXiv e-prints, arXiv:2106.15075.
<https://arxiv.org/abs/2106.15075>
- Belczynski, K., Klencki, J., Fields, C. E., et al. 2020, *A&A*, 636, A104, doi: [10.1051/0004-6361/201936528](https://doi.org/10.1051/0004-6361/201936528)
- Blandford, R. D., & Znajek, R. L. 1977, *MNRAS*, 179, 433, doi: [10.1093/mnras/179.3.433](https://doi.org/10.1093/mnras/179.3.433)
- Broekgaarden, F. S., Berger, E., Neijssel, C. J., et al. 2021, arXiv e-prints, arXiv:2103.02608.
<https://arxiv.org/abs/2103.02608>
- Cheng, K. S., & Wang, J.-M. 1999, *ApJ*, 521, 502, doi: [10.1086/307572](https://doi.org/10.1086/307572)
- Coughlin, M., Dietrich, T., Kawaguchi, K., et al. 2017, *ApJ*, 849, 12, doi: [10.3847/1538-4357/aa9114](https://doi.org/10.3847/1538-4357/aa9114)
- Coughlin, M. W., Kasliwal, M. M., Perley, D. A., et al. 2019, *GRB Coordinates Network*, 24283, 1
- Coughlin, M. W., Dietrich, T., Antier, S., et al. 2020a, *MNRAS*, 497, 1181, doi: [10.1093/mnras/staa1925](https://doi.org/10.1093/mnras/staa1925)
- . 2020b, *MNRAS*, 492, 863, doi: [10.1093/mnras/stz3457](https://doi.org/10.1093/mnras/stz3457)
- Coulter, D. A., Foley, R. J., Kilpatrick, C. D., et al. 2017, *Science*, 358, 1556, doi: [10.1126/science.aap9811](https://doi.org/10.1126/science.aap9811)
- Cowperthwaite, P. S., Berger, E., Villar, V. A., et al. 2017, *ApJL*, 848, L17, doi: [10.3847/2041-8213/aa8fc7](https://doi.org/10.3847/2041-8213/aa8fc7)
- Dai, Z. G. 2019, *ApJL*, 873, L13, doi: [10.3847/2041-8213/ab0b45](https://doi.org/10.3847/2041-8213/ab0b45)
- Darbha, S., Kasen, D., Foucart, F., & Price, D. J. 2021, arXiv e-prints, arXiv:2103.03378.
<https://arxiv.org/abs/2103.03378>
- Dietrich, T., Coughlin, M. W., Pang, P. T. H., et al. 2020, *Science*, 370, 1450, doi: [10.1126/science.abb4317](https://doi.org/10.1126/science.abb4317)
- Drout, M. R., Piro, A. L., Shappee, B. J., et al. 2017, *Science*, 358, 1570, doi: [10.1126/science.aag0049](https://doi.org/10.1126/science.aag0049)
- Drozda, P., Belczynski, K., O’Shaughnessy, R., Bulik, T., & Fryer, C. L. 2020, arXiv e-prints, arXiv:2009.06655.
<https://arxiv.org/abs/2009.06655>
- Eichler, D., Livio, M., Piran, T., & Schramm, D. N. 1989, *Nature*, 340, 126, doi: [10.1038/340126a0](https://doi.org/10.1038/340126a0)
- Evans, P. A., Cenko, S. B., Kennea, J. A., et al. 2017, *Science*, 358, 1565, doi: [10.1126/science.aap9580](https://doi.org/10.1126/science.aap9580)
- Fernández, R., & Metzger, B. D. 2013, *MNRAS*, 435, 502, doi: [10.1093/mnras/stt1312](https://doi.org/10.1093/mnras/stt1312)
- Foucart, F. 2012, *PhRvD*, 86, 124007, doi: [10.1103/PhysRevD.86.124007](https://doi.org/10.1103/PhysRevD.86.124007)
- Foucart, F., Hinderer, T., & Nissanke, S. 2018, *PhRvD*, 98, 081501 (F18), doi: [10.1103/PhysRevD.98.081501](https://doi.org/10.1103/PhysRevD.98.081501)
- Foucart, F., Deaton, M. B., Duez, M. D., et al. 2013, *PhRvD*, 87, 084006, doi: [10.1103/PhysRevD.87.084006](https://doi.org/10.1103/PhysRevD.87.084006)
- Fragione, G., & Loeb, A. 2021, *MNRAS*, 503, 2861, doi: [10.1093/mnras/stab666](https://doi.org/10.1093/mnras/stab666)
- Fujibayashi, S., Shibata, M., Wanajo, S., et al. 2020a, *PhRvD*, 101, 083029, doi: [10.1103/PhysRevD.101.083029](https://doi.org/10.1103/PhysRevD.101.083029)
- . 2020b, arXiv e-prints, arXiv:2009.03895.
<https://arxiv.org/abs/2009.03895>
- Fuller, J., & Ma, L. 2019, *ApJL*, 881, L1, doi: [10.3847/2041-8213/ab339b](https://doi.org/10.3847/2041-8213/ab339b)
- Gao, H., Ai, S.-K., Cao, Z.-J., et al. 2020, *Frontiers of Physics*, 15, 24603, doi: [10.1007/s11467-019-0945-9](https://doi.org/10.1007/s11467-019-0945-9)
- Ghirlanda, G., Salafia, O. S., Paragi, Z., et al. 2019, *Science*, 363, 968, doi: [10.1126/science.aau8815](https://doi.org/10.1126/science.aau8815)
- Giacobbo, N., & Mapelli, M. 2018, *MNRAS*, 480, 2011, doi: [10.1093/mnras/sty1999](https://doi.org/10.1093/mnras/sty1999)
- Godzieba, D. A., Radice, D., & Bernuzzi, S. 2020, arXiv e-prints, arXiv:2007.10999.
<https://arxiv.org/abs/2007.10999>
- Goldstein, A., Veres, P., Burns, E., et al. 2017, *ApJL*, 848, L14, doi: [10.3847/2041-8213/aa8f41](https://doi.org/10.3847/2041-8213/aa8f41)
- Goldstein, A., Hamburg, R., Wood, J., et al. 2019a, arXiv e-prints, arXiv:1903.12597.
<https://arxiv.org/abs/1903.12597>
- Goldstein, D. A., Andreoni, I., Nugent, P. E., et al. 2019b, *ApJL*, 881, L7, doi: [10.3847/2041-8213/ab3046](https://doi.org/10.3847/2041-8213/ab3046)
- Gompertz, B. P., Cutter, R., Steeghs, D., et al. 2020, *MNRAS*, 497, 726, doi: [10.1093/mnras/staa1845](https://doi.org/10.1093/mnras/staa1845)
- Graham, M. J., Kulkarni, S. R., Bellm, E. C., et al. 2019, *PASP*, 131, 078001, doi: [10.1088/1538-3873/ab006c](https://doi.org/10.1088/1538-3873/ab006c)
- Hosseinzadeh, G., Cowperthwaite, P. S., Gomez, S., et al. 2019, *ApJL*, 880, L4, doi: [10.3847/2041-8213/ab271c](https://doi.org/10.3847/2041-8213/ab271c)
- Just, O., Bauswein, A., Ardevol Pulpillo, R., Goriely, S., & Janka, H. T. 2015, *MNRAS*, 448, 541, doi: [10.1093/mnras/stv009](https://doi.org/10.1093/mnras/stv009)
- Kasen, D., Metzger, B., Barnes, J., Quataert, E., & Ramirez-Ruiz, E. 2017, *Nature*, 551, 80, doi: [10.1038/nature24453](https://doi.org/10.1038/nature24453)
- Kasliwal, M. M., Nakar, E., Singer, L. P., et al. 2017, *Science*, 358, 1559, doi: [10.1126/science.aap9455](https://doi.org/10.1126/science.aap9455)

- Kasliwal, M. M., Anand, S., Ahumada, T., et al. 2020, arXiv e-prints, arXiv:2006.11306.
<https://arxiv.org/abs/2006.11306>
- Kawaguchi, K., Kyutoku, K., Shibata, M., & Tanaka, M. 2016, *ApJ*, 825, 52 (K16),
doi: [10.3847/0004-637X/825/1/52](https://doi.org/10.3847/0004-637X/825/1/52)
- Kawaguchi, K., Shibata, M., & Tanaka, M. 2020a, *ApJ*, 893, 153, doi: [10.3847/1538-4357/ab8309](https://doi.org/10.3847/1538-4357/ab8309)
- . 2020b, *ApJ*, 889, 171, doi: [10.3847/1538-4357/ab61f6](https://doi.org/10.3847/1538-4357/ab61f6)
- Kiel, P. D., Hurley, J. R., Bailes, M., & Murray, J. R. 2008, *MNRAS*, 388, 393, doi: [10.1111/j.1365-2966.2008.13402.x](https://doi.org/10.1111/j.1365-2966.2008.13402.x)
- Kilpatrick, C. D., Foley, R. J., Kasen, D., et al. 2017, *Science*, 358, 1583, doi: [10.1126/science.aag0073](https://doi.org/10.1126/science.aag0073)
- Kilpatrick, C. D., Coulter, D. A., Arcavi, I., et al. 2021, arXiv e-prints, arXiv:2106.06897.
<https://arxiv.org/abs/2106.06897>
- Krüger, C. J., & Foucart, F. 2020, *PhRvD*, 101, 103002 (KF20), doi: [10.1103/PhysRevD.101.103002](https://doi.org/10.1103/PhysRevD.101.103002)
- Kyutoku, K., Ioka, K., Okawa, H., Shibata, M., & Taniguchi, K. 2015, *PhRvD*, 92, 044028,
doi: [10.1103/PhysRevD.92.044028](https://doi.org/10.1103/PhysRevD.92.044028)
- Kyutoku, K., Ioka, K., & Shibata, M. 2013, *PhRvD*, 88, 041503, doi: [10.1103/PhysRevD.88.041503](https://doi.org/10.1103/PhysRevD.88.041503)
- Kyutoku, K., Okawa, H., Shibata, M., & Taniguchi, K. 2011, *PhRvD*, 84, 064018,
doi: [10.1103/PhysRevD.84.064018](https://doi.org/10.1103/PhysRevD.84.064018)
- Lattimer, J. M., & Schramm, D. N. 1974, *ApJL*, 192, L145,
doi: [10.1086/181612](https://doi.org/10.1086/181612)
- . 1976, *ApJ*, 210, 549, doi: [10.1086/154860](https://doi.org/10.1086/154860)
- Lazzati, D., Perna, R., Morsony, B. J., et al. 2018, *PhRvL*, 120, 241103, doi: [10.1103/PhysRevLett.120.241103](https://doi.org/10.1103/PhysRevLett.120.241103)
- Li, L.-X., & Paczyński, B. 1998, *ApJL*, 507, L59,
doi: [10.1086/311680](https://doi.org/10.1086/311680)
- Li, Y., & Shen, R.-F. 2021, *ApJ*, 911, 87,
doi: [10.3847/1538-4357/abe462](https://doi.org/10.3847/1538-4357/abe462)
- LSST Science Collaboration, Abell, P. A., Allison, J., et al. 2009, arXiv e-prints, arXiv:0912.0201.
<https://arxiv.org/abs/0912.0201>
- Lyman, J. D., Lamb, G. P., Levan, A. J., et al. 2018, *Nature Astronomy*, 2, 751, doi: [10.1038/s41550-018-0511-3](https://doi.org/10.1038/s41550-018-0511-3)
- Ma, S.-B., Lei, W.-H., Gao, H., et al. 2018, *ApJL*, 852, L5,
doi: [10.3847/2041-8213/aaa0cd](https://doi.org/10.3847/2041-8213/aaa0cd)
- Manchester, R. N., Hobbs, G. B., Teoh, A., & Hobbs, M. 2005, *AJ*, 129, 1993, doi: [10.1086/428488](https://doi.org/10.1086/428488)
- Margutti, R., Berger, E., Fong, W., et al. 2017, *ApJL*, 848, L20, doi: [10.3847/2041-8213/aa9057](https://doi.org/10.3847/2041-8213/aa9057)
- McKernan, B., Ford, K. E. S., & O’Shaughnessy, R. 2020, *MNRAS*, 498, 4088, doi: [10.1093/mnras/staa2681](https://doi.org/10.1093/mnras/staa2681)
- Metzger, B. D., Martínez-Pinedo, G., Darbha, S., et al. 2010, *MNRAS*, 406, 2650,
doi: [10.1111/j.1365-2966.2010.16864.x](https://doi.org/10.1111/j.1365-2966.2010.16864.x)
- Miller, M. C., Lamb, F. K., Dittmann, A. J., et al. 2021, arXiv e-prints, arXiv:2105.06979.
<https://arxiv.org/abs/2105.06979>
- Müller, H., & Serot, B. D. 1996, *NuPhA*, 606, 508,
doi: [10.1016/0375-9474\(96\)00187-X](https://doi.org/10.1016/0375-9474(96)00187-X)
- Narayan, R., Paczynski, B., & Piran, T. 1992, *ApJL*, 395, L83, doi: [10.1086/186493](https://doi.org/10.1086/186493)
- Ośłowski, S., Bulik, T., Gondek-Rosińska, D., & Belczyński, K. 2011, *MNRAS*, 413, 461,
doi: [10.1111/j.1365-2966.2010.18147.x](https://doi.org/10.1111/j.1365-2966.2010.18147.x)
- Paczynski, B. 1991, *AcA*, 41, 257
- Page, K. L., Evans, P. A., Tohuvavohu, A., et al. 2020, *MNRAS*, doi: [10.1093/mnras/staa3032](https://doi.org/10.1093/mnras/staa3032)
- Perego, A., Radice, D., & Bernuzzi, S. 2017, *ApJL*, 850, L37, doi: [10.3847/2041-8213/aa9ab9](https://doi.org/10.3847/2041-8213/aa9ab9)
- Perna, R., Lazzati, D., & Cantiello, M. 2021, *ApJL*, 906, L7, doi: [10.3847/2041-8213/abd319](https://doi.org/10.3847/2041-8213/abd319)
- Pian, E., D’Avanzo, P., Benetti, S., et al. 2017, *Nature*, 551, 67, doi: [10.1038/nature24298](https://doi.org/10.1038/nature24298)
- Qin, Y., Fragos, T., Meynet, G., et al. 2018, *A&A*, 616, A28, doi: [10.1051/0004-6361/201832839](https://doi.org/10.1051/0004-6361/201832839)
- Riley, T. E., Watts, A. L., Bogdanov, S., et al. 2019, *ApJL*, 887, L21, doi: [10.3847/2041-8213/ab481c](https://doi.org/10.3847/2041-8213/ab481c)
- Rosswog, S. 2007, *MNRAS*, 376, L48,
doi: [10.1111/j.1745-3933.2007.00284.x](https://doi.org/10.1111/j.1745-3933.2007.00284.x)
- Sagués Carracedo, A., Bulla, M., Feindt, U., & Goobar, A. 2020, arXiv e-prints, arXiv:2004.06137.
<https://arxiv.org/abs/2004.06137>
- Savchenko, V., Ferrigno, C., Kuulkers, E., et al. 2017, *ApJL*, 848, L15, doi: [10.3847/2041-8213/aa8f94](https://doi.org/10.3847/2041-8213/aa8f94)
- Shibata, M., & Taniguchi, K. 2011, *Living Reviews in Relativity*, 14, 6, doi: [10.12942/lrr-2011-6](https://doi.org/10.12942/lrr-2011-6)
- Siegel, D. M., & Metzger, B. D. 2017, *PhRvL*, 119, 231102, doi: [10.1103/PhysRevLett.119.231102](https://doi.org/10.1103/PhysRevLett.119.231102)
- Smartt, S. J., Chen, T. W., Jerkstrand, A., et al. 2017, *Nature*, 551, 75, doi: [10.1038/nature24303](https://doi.org/10.1038/nature24303)
- Sridhar, N., Zrake, J., Metzger, B. D., Sironi, L., & Giannios, D. 2021, *MNRAS*, 501, 3184,
doi: [10.1093/mnras/staa3794](https://doi.org/10.1093/mnras/staa3794)
- Stachie, C., Coughlin, M. W., Dietrich, T., et al. 2021, *MNRAS*, 505, 4235, doi: [10.1093/mnras/stab1492](https://doi.org/10.1093/mnras/stab1492)
- Tanaka, M., Utsumi, Y., Mazzali, P. A., et al. 2017, *PASJ*, 69, 102, doi: [10.1093/pasj/psx121](https://doi.org/10.1093/pasj/psx121)
- Thakur, A. L., Dichiara, S., Troja, E., et al. 2020, *MNRAS*, 499, 3868, doi: [10.1093/mnras/staa2798](https://doi.org/10.1093/mnras/staa2798)

- The LIGO Scientific Collaboration, the Virgo Collaboration, Abbott, R., et al. 2020a, arXiv e-prints, arXiv:2010.14550. <https://arxiv.org/abs/2010.14550>
- . 2020b, arXiv e-prints, arXiv:2010.14533. <https://arxiv.org/abs/2010.14533>
- Troja, E., Piro, L., van Eerten, H., et al. 2017, *Nature*, 551, 71, doi: [10.1038/nature24290](https://doi.org/10.1038/nature24290)
- Typel, S., Röpke, G., Klähn, T., Blaschke, D., & Wolter, H. H. 2010, *PhRvC*, 81, 015803, doi: [10.1103/PhysRevC.81.015803](https://doi.org/10.1103/PhysRevC.81.015803)
- Villar, V. A., Guillochon, J., Berger, E., et al. 2017, *ApJL*, 851, L21, doi: [10.3847/2041-8213/aa9c84](https://doi.org/10.3847/2041-8213/aa9c84)
- Yang, Y.-S., Zhong, S.-Q., Zhang, B.-B., et al. 2020, *ApJ*, 899, 60, doi: [10.3847/1538-4357/ab9ff5](https://doi.org/10.3847/1538-4357/ab9ff5)
- Zappa, F., Bernuzzi, S., Pannarale, F., Mapelli, M., & Giacobbo, N. 2019, *PhRvL*, 123, 041102, doi: [10.1103/PhysRevLett.123.041102](https://doi.org/10.1103/PhysRevLett.123.041102)
- Zhang, B. 2019, *ApJL*, 873, L9, doi: [10.3847/2041-8213/ab0ae8](https://doi.org/10.3847/2041-8213/ab0ae8)
- Zhang, B. B., Zhang, B., Sun, H., et al. 2018, *Nature Communications*, 9, 447, doi: [10.1038/s41467-018-02847-3](https://doi.org/10.1038/s41467-018-02847-3)
- Zhang, N.-B., & Li, B.-A. 2020, *ApJ*, 902, 38, doi: [10.3847/1538-4357/abb470](https://doi.org/10.3847/1538-4357/abb470)
- Zhu, J.-P., Wang, K., & Zhang, B. 2021a, arXiv e-prints, arXiv:2107.06070. <https://arxiv.org/abs/2107.06070>
- Zhu, J.-P., Wang, K., Zhang, B., et al. 2021b, *ApJL*, 911, L19, doi: [10.3847/2041-8213/abf2c3](https://doi.org/10.3847/2041-8213/abf2c3)
- Zhu, J.-P., Yang, Y.-P., Liu, L.-D., et al. 2020a, *ApJ*, 897, 20 (Z20), doi: [10.3847/1538-4357/ab93bf](https://doi.org/10.3847/1538-4357/ab93bf)
- Zhu, J.-P., Zhang, B., Yu, Y.-W., & Gao, H. 2021c, *ApJL*, 906, L11, doi: [10.3847/2041-8213/abd412](https://doi.org/10.3847/2041-8213/abd412)
- Zhu, J.-P., Wu, S., Yang, Y.-P., et al. 2020b, arXiv e-prints, arXiv:2011.02717. <https://arxiv.org/abs/2011.02717>